B. Kämpfer, O.P. Pavlenko, M.I. Gorenstein

A. Peshier, G. Soff

Rapidity dependence of thermal dileptons resulting from hadronizing quark-gluon matter with finite baryon charge

Forschungszentrum Rossendorf e.V.

Postfach 51 01 19 · D-01314 Dresden

Bundesrepublik Deutschland

Telefon (0351) 591 3258

Rapidity dependence of thermal dileptons resulting from hadronizing quark-gluon matter with finite baryon charge

B. KÄMPFER[1,2], O.P. PAVLENKO[1,3], M.I. GORENSTEIN[3],
A. PESHIER[2], G. SOFF[2]

[1]Research Center Rossendorf, PF 510119, 01314 Dresden, Germany
[2]Institut für Theoretische Physik, TU Dresden,
Mommsenstr. 13, 01062 Dresden, Germany
[3]Institut for Theoretical Physics, 252 143 Kiev, Ukraine

Abstract: The influence of a non-vanishing baryon charge on the rapidity distribution of dileptons produced in ultrarelativistic heavy-ion collisions is studied. We employ a frozen motion model with scaling invariant expansion of the hadronizing quark-gluon plasma as well as a realistic rapidity distribution of secondary particles (i.e., pions and baryons) expected for RHIC energies. We find a considerable suppression of the dilepton production yield at large rapidities due to the finite baryon density. To discriminate the thermal dileptons from Drell-Yan background we propose to utilize the dilepton yield scaled suitably by the pion multiplicity as function of rapidity.

I. Introduction

Dileptons still represent a promising probe of deconfined matter in the course of central ultrarelativistic heavy-ion collisions [1, 2, 3]. As indicated by many authors [3, 4, 5] the dilepton spectrum at moderately high invariant pair masses of about 2 - 4 GeV is most appropriate for the determination of the initial stage of matter. In particular if a thermalized quark-gluon plasma is formed, the dilepton yield is sensitive to its initial temperature. (Effects of pre-equilibrium and thermalization are considered in Ref. [6].)

Due to considerable contributions to the dilepton spectra from initial hard parton collisions (i.e., the Drell-Yan background) and decays of charmed particles just in the intermediate invariant mass region one is forced to look for more refined characteristics related to the dilepton production processes in order to separate thermal emission sources from the background. One possibility is considered in Ref. [7] by using the correlation between dilepton production and rapidity density of pions in the central rapidity region.

The long series of predicted dilepton spectra predominatly is based on Bjorken's evolutionary scenario of matter, i.e., flat rapidity distributions and vanishing baryon charge in the central region. The present experiments at AGS in Brookhaven and SPS in CERN, however, show a clear distinction to this: There is a large degree of baryon stopping (implying a large baryon charge in and around the central region) and pronounced Gaussian like distributions of secondary particles [8].

An attempt to reveal on realistic rapidity distributions of pions is made recently in Ref. [9], and the rapidity dependence of dileptons is proposed as possible tool to distinguish the thermal plasma source from background. The main assumptions used in Ref. [9] are: longitudinal scaling expansion of matter and the Gaussian distribution of secondary pions as predicted for RHIC and LHC energies. Using a bag model equation of state for baryon-free matter one can deduce the rapidity dependence of the initial temperature. The rapidity distribution of dileptons from thermalized matter depends sensitively on the initial temperature distribution and, thus, deviates considerably from Drell-Yan and charm decay background.

While the scaling expansion of the matter formed in high-energy nuclear collisions is generally believed to represent a good approximation, the neglect of the

baryons requires an improvement, even for RHIC and LHC energies, where advanced microscopic transport models [10, 11] predict still considerably high baryon density in a wide rapidity region. This finite baryon density implies also a finite baryon chemical potential. As demonstrated in Ref. [12] such a finite baryon chemical potential leads to noticeable suppression of the dilepton rate from the quark-gluon plasma, if matter states with the same energy density are compared.

Additionally to the experimental observation there is also an "theoretical" objective to include a finite chemical potential into the consideration within the framework of the scaling model. It is easy to verify that scaling solutions (e.g., $v_z = z/t$) do not satisfy hydrodynamical equations for a vanishing chemical potential while the other thermodynamical parameters are rapidity dependent.

In the present paper we consider the influence of the finite baryon density on the rapidity distribution of dileptons resulting from a hadronizing quark-gluon plasma. We assume the validity of the frozen motion model, i.e., a longitudinal scaling expansion and conservation of the entropy per baryon in a comoving volume element during the adiabatic expansion of the matter up to freeze out. With this at hand we deduce the initial rapidity distribution of the temperature and the baryon chemical potential from the RQMD calculations [10] for the final distributions of pions and baryons in nuclear collisions at RHIC energies. For a realistic comparison with expected experimental data we analyze the dilepton yield over the whole space-time history of the radiating matter, including a possible mixed phase and hadron matter. A comparison with the Drell-Yan background is provided, and the shape of the correlation between dileptons and pion multiplicity is predicted.

Our paper is organized as follows. In section 2 we present the initial conditions and the equation of state. The thermal dilepton rates for matter with baryon charge and the Drell-Yan background are calculated in section 3. Numerical results are discussed in section 4 for various baryon rapidity distributions and for a Gaussian pion distribution. Our results are summarized in section 5.

II. Initial conditions and equation of state

To be specific we assume that initially the matter is in an equilibrated deconfined state. As equation of state we employ the standard bag model for u,d quarks and

gluons

$$e(\mu_q, T) = \frac{37\pi^2}{30}T^4 + 3T^2\mu_q^2 + \frac{3}{2\pi^2}\mu_q^4 + B, \tag{1}$$

$$p(\mu_q, T) = \frac{1}{3}e - \frac{4}{3}B, \tag{2}$$

$$s(\mu_q, T) = \frac{4}{3}\frac{37\pi^2}{30}T^3 + 2T\mu_q^2, \tag{3}$$

$$n(\mu_q, T) = \frac{2}{3}\left(T^2\mu_q + \frac{1}{\pi^2}\mu_q^3\right), \tag{4}$$

where e, p, s, n, T, μ_q denote the energy density, pressure, entropy density, baryon density, temperature and quark chemical potential of the quark-gluon matter, respectively. The value of the bag constant is chosen to be $B^{1/4} = 235$ MeV. We employ units with $\hbar = c = 1$.

The results of Ref. [10] for the rapidity density of secondary pions dN_π/dy for heavy-ion collisions at RHIC energy can be approximated by

$$\frac{dN_\pi}{dy} = N_0 \exp\left\{-\frac{y^2}{2\sigma^2}\right\} \tag{5}$$

with $N_0 = 1200$, $\sigma = 2.4$ in the rapidity interval $|y| \le 4$. This holds for symmetric AA collisions with A ≈ 200.

The entropy distribution is mainly related to pions. Since for the ideal scaling expansion the entropy is conserved in a comoving fluid element, one can derive from the pion number density distribution (5) the initial entropy density distribution

$$s_0(y) = \frac{N_0}{0.27\pi R^2 \tau_0} \exp\left\{-\frac{y^2}{2\sigma^2}\right\}, \tag{6}$$

where R is the transverse radius of the system and τ_0 is the beginning of the scaling expansion of the thermalized matter.

In order to find the rapidity dependence of the initial temperature $T_0(y)$ one needs in addition to eq. (6) the rapidity distributions of baryons. The RQMD results of Ref. [10] allow to extract a rough fit for the ratio $\xi \equiv \mu_q/T$: $\xi(y) = by^a$ with $a = 1.8$ and $b = 0.15$. This parametrization has at mid-rapidity no baryon charge, as e.g. predicted by the parton kinetic model [13], while Ref. [10] exhibits a small contribution there. (Below we comment on the effect of baryon charge at mid-rapidity.) Therefore the initial temperature distributions reads

$$T_0(y) = \left[s_0(y)\left\{\frac{4}{3}\frac{37\pi^2}{30} + 2b^2y^{2a}\right\}^{-1}\right]^{1/3}. \tag{7}$$

4

As in the frozen motion model by Shuryak and Xiong [18] we assume that the scaling properties of the Bjorken scenario can be applied, i.e., $\tau s = const$, and that the rapidity of a matter element is not changed during the expansion. (For the first tens fm/c this is an excellent approximation. We verified this by solving the hydrodynamical evolution equations for the case $e = 3p$ and $\mu = 0$. The presence of the chemical potential additionally reduces the rapidity-driving pressure gradient.) This neglects also transverse expansion, which becomes important only in the late stages. As the second governing equation we choose the adiabaticity condition $s/n = const$.

Having now specified the initial conditions we can proceed with the approximate dynamics. The dynamical path of matter is determined by the above conditions. The special form of the quark-gluon equation of state determines the states of deconfined matter by $\xi(\tau) = const$ and $T(\tau, y) = T_0(y)(\tau_0/\tau)^{1/3}$. This behavior is changed in the mixed phase and, of course, in the hadron phase.

To model the confinement transition we employ a hadron gas equation of state with excluded volume effects which account for the finite hadron sizes [14, 15]. It relies on an ideal gas approximation of pions, nucleons and anti-nucleons, i.e,

$$p^{id}(\mu, T) = \frac{\pi^2}{30}T^4 + \frac{4}{\pi^2}m^2T^2 \sum_{l=1}^{\infty} \frac{(-1)^{l+1}}{l^2} \mathrm{ch}\left(\frac{\mu}{T}l\right) K_2\left(\frac{m}{T}l\right), \tag{8}$$

$$s^{id}(\mu, T) = \frac{2\pi^2}{15}T^3 + \frac{4}{\pi^2}m^2 \left[\sum_{l=1}^{\infty}(-1)^{l+1}\mathrm{ch}\left(\frac{\mu}{T}l\right)\left\{4l^{-2}K_2\left(\frac{m}{T}l\right)T + l^{-1}K_1\left(\frac{m}{T}l\right)m\right\} \right.$$
$$\left. - \frac{\mu}{T}n^{id}(\mu, T)\right] \tag{9}$$

$$n^{id}(\mu, T) = \frac{4}{\pi^2}m^2T \sum_{l=1}^{\infty} \frac{(-1)^l}{l+1} \mathrm{sh}\left(\frac{\mu}{T}l\right) K_2\left(\frac{m}{T}l\right), \tag{10}$$

where μ is the hadronic baryon chemical potential ($\mu = 3\mu_q \equiv \mu_B$), and $m = 939$ MeV stands for the nucleon mass. This expansion is valid for $\mu < m$. Pions are here approximated by massless particles, and $K_{1,2}$ denote modified Bessel functions. In the framework of the approach of Refs. [14, 15] one has to divide all the above hadronic thermodynamical quantities by $1 + n^{id}(\mu, T) V_0$ with $V_0 = \frac{4}{3}\pi R_0^3$ ($R_0 = 0.8$ fm), e.g., $p = p^{id} / (1 + n^{id} V_0)$. By this procedure one takes into account the finite hadron size and simulates interactions. Such an approximation is known [16] to be thermodynamically not fully self-consistent, but may serve as useful parametrization

for our dilepton estimates from the mixed phase. (The fully thermodynamically self-consistent approach in Ref. [16] relies on a modified [on the particle level] chemical potential which is proportional to the pressure; this approach is too unhandy here.) The phase boundaries are constructed from Gibbs conditions of phase equilibrium $p_q(\mu_q, T) = p_h(\mu, T)$. These phase boundaries and the dynamical paths of fluid elements throughout the temperature - density plane are displayed in Fig. 1. The depicted paths correspond, according to our evolutionary propositions, to various rapidities. The reheating in the mixture region [17] due to released latent heat already has been established some time ago as well as the focusing of the paths in the hadronic states.

III. Dilepton yield

The dilepton yield from the quark-gluon matter due to the dominating quark fusion process $q\bar{q} \rightarrow l\bar{l}$ can be written in the form ($M \gg T$)

$$\frac{dN_{l\bar{l}}^Q}{d^4x \, dM_\perp^2 \, dM^2 dY} = \frac{\alpha^2}{8\pi^3} F_q \exp\left\{-\frac{M_\perp \mathrm{ch}(Y - \eta)}{T}\right\} J_q, \quad (11)$$

where $q^\mu = (M_\perp \mathrm{ch}Y, \vec{q}_\perp, M_\perp \mathrm{sh}Y)$ is the four momentum of lepton pairs with rapidity Y, invariant mass M, and transverse mass $M_\perp = \sqrt{M^2 + q_\perp^2}$ ($\vec{q}_\perp$ is the transverse momentum). $F_q = \frac{5}{9}$ is the formfactor for u,d quarks, and η denotes the flow rapidity for which $d^4x = \pi R^2 \tau d\tau d\eta$. J_q is determined by

$$
\begin{aligned}
J_q &= T(M_\perp^2 \mathrm{ch}^2[Y - \eta] - M^2)^{-1/2} \ln \frac{(\exp\{\frac{E_+}{T}\} + Z)(\exp\{-\frac{E_+}{T}\} + Z)}{(\exp\{\frac{E_-}{T}\} + Z)(\exp\{-\frac{E_-}{T}\} + Z)}, \quad (12)\\
E_\pm &= \frac{1}{2}\left[M_\perp \mathrm{ch}(Y - \eta) \pm \sqrt{M_\perp^2 \mathrm{ch}^2(Y - \eta) - M^2}\right],\\
Z &= \exp\left(-\frac{\mu_q}{T}\right).
\end{aligned}
$$

The factor J_q appears just because of the non-zero baryon chemical potential of quarks $\mu_q \neq 0$. In the pure quark-gluon plasma phase the ratio $\xi = \mu_q/T$ depends only on the rapidity η.

Our calculations of the dilepton production yield from the hadron phase are based on the reaction $\pi^+\pi^- \rightarrow \rho \rightarrow l\bar{l}$. Other processes like $\pi N \rightarrow N + l\bar{l}$, $\pi N \rightarrow \Delta + l\bar{l}$ (with N, Δ in intermediate states) and $N\bar{N} \rightarrow l\bar{l}$ are estimated to provide smaller contributions to the dilepton rate, at least in the intermediate invariant mass region

[2]. Modifications of the pion annihilation source by higher resonances (in particular the a_1 contributions) are discussed in Refs. [18]. It should be pointed out also that a complete consideration of the hadron gas contributions to the dilepton yield needs the regard of the transverse expansion. As well known [5] the life time of the hadron stage is shortened by the transverse flow, and accordingly the contributions to the electromagnetic probes would be not so strong as predicted in the purely longitudinal expansion scenario [19]. The rate from the pion annihilation process reads

$$\frac{dN_{ll}^{\pi}}{d^4x\, dM_{\perp}^2\, dM^2\, dY} = \frac{\alpha^2}{8\pi^3} F_h \exp\left\{-\frac{M_{\perp}\mathrm{ch}(Y-\eta)}{T}\right\}, \qquad (13)$$

with $F_h = \frac{1}{12}m_{\rho}^4 \left[(m_{\rho}^2 - M^2)^2 + m_{\rho}^2\Gamma_{\rho}^2\right]^{-1}$, ($m_{\rho} = 0.77$ GeV, $\Gamma_{\rho} = 0.15$ GeV).

To integrate the rates (11, 13) over space-time and to obtain the total yield we use the approximation $\exp\{-\frac{M_{\perp}}{T}\mathrm{ch}(Y-\eta)\} \approx \exp\{-\frac{M_{\perp}}{T}\}\sqrt{\frac{2\pi T}{M_{\perp}}}\delta(Y-\eta)$ that leads to

$$\frac{dN_{ll}}{dM_{\perp}^2\, dM^2\, dY} = \frac{\alpha^2 R^2}{8\pi^2}\sqrt{\frac{2\pi}{M_{\perp}}}\int_{\tau_0} d\tau\, \tau\sqrt{T}\exp\left\{-\frac{M_{\perp}}{T}\right\}\left[xF_qJ_q + (1-x)F_h\right], \quad (14)$$

where x is the volume fraction of the deconfined matter ($x = 1[0]$ for pure quark [hadron] matter). The integration is performed along the dynamical paths, as displayed in Fig. 1, which are determined by the rapidity. As initial time we use the standard values $\tau_0 = 0.25 - 1$ fm/c. (Another choice such as $\tau_0 \propto 1/T_0$ does not lead to deviating results.) We also restrict ourselves mainly to the consideration of the deconfined phase and the mixed phase.

Now we discuss the dilepton production through initial hard parton collisions (Drell-Yan background). Our calculations of the rapidity dependence of Drell-Yan pairs in central collisions are based on the Duke-Owens structure functions 1.1 [20] and

$$\frac{dN_{ll}^{DY}}{dM^2\, dY} = \frac{A^{4/3}}{\pi r_0^2}\mathcal{K}\frac{2\pi\alpha^2}{81M^4}\left[5(V(x_a)S(x_b) + S(x_a)V(x_b)) + 24S(x_a)S(x_b)\right] \qquad (15)$$

(cf. [9]; $V(x) = xv(x)$ is the valence quark structure function, while $S(x) = xs(x)$ refers to the sea quarks; $r_0 = 1.2$ fm) with $x_{a,b} = M\exp\{\pm Y\}/\sqrt{s}$. The usual factor $\mathcal{K} = 2$ accounts for higher order corrections.

7

IV. Results

The results of our calculations of the dilepton rapidity distributions of the yield $dN_{l\bar{l}}/dM_\perp^2\, dM^2\, dY$ for $M = 3$ GeV and $M_\perp = 4$ GeV are shown in Fig. 2. One observes a considerable suppression (by about a factor of 10) of the yield from baryon-rich matter in the high rapidity region $Y \sim 4$, compared to the case with vanishing baryon charge $n_B = 0$. For the pure quark-gluon plasma contribution the suppression is even stronger. The reason for this is that for a fixed initial energy density state a non-zero chemical potential leads to a decreasing initial temperature which determines sensitively the dilepton rate. If we consider states of quark-gluon plasma with the same temperature but different baryon-chemical potential, then the dilepton spectrum does not depend so sensitively on μ due to the weaker logarithmic dependence in eq. (12). This can be deduced from Fig. 2 for $|Y| \le 2$, where the high pion rapidity density dominates over variations of the baryon distribution; in fact there one has $\xi < 1$, and a negligible effect of the baryon charge. Therefore the influence of the baryon chemical potential is not so trivial, but mediated through both the equation of state and the initial temperature. (Similar arguments can be applied to the Compton like process, because a lower initial temperature causes a suppressed gluon density.) It is also obvious from Fig. 2 that the contribution of the mixed phase becomes important only in the interval $|Y| > 2$.

This conclusion can be also important for SPS Pb + Pb collisions where a high stopping power is expected, and the rapidity distribution of baryons might be similar as the pion distribution. In this case the dilepton yield in the central region is suppressed (compared to the baryon-free case) but the shape of the rapidity distribution is not noticeably modified. To be specific we assume for the moment being $dN_B/dy = \mathcal{N}_B dN_\pi/dy$ with $\mathcal{N}_B = 6.1 \cdot 10^{-2}$ from the normalization to 400 baryons in the rapidity interval $|y| \le 4$. In this case ξ is independent of rapidity and consequently we find in our scaling approach a depletion of the initial temperature only by 3 MeV (for $\tau_0 = 0.25$ fm/c) compared to the case of vanishing baryon charge. This is, of course, negligible for the dilepton rate which is most sensitive to the temperature. If the pion rapidity density is not so large, then a more important suppression of dilepton yield would appear. The above simple estimates are based on the qualitative dependence of the initial temperature on pion and baryon rapidity

8

distributions and would remain valid for more involved dynamical model including the specific high stopping power regime.

Let us now return to the RHIC expectations. The $M_\perp$-integrated yield is displayed in Figs. 3a and 3b for pairs with invariant mass $M = 3$ GeV and $\tau_0 = 0.5$ and 1 fm/c. The above obtained suppression due to the non-zero baryon density in the fragmentation region remains valid also in these spectra. Fig. 3a compares the yields for different initial temperatures (caused by different values of τ_0, cf. eqs. (6,7)) and illustrates the contributions of the quark-gluon plasma to the total yield. For shorter initial time ($\tau_0 = 0.5$ fm/c) the initial temperature would be estimated as higher, and the quark-gluon plasma contribution dominates even at high rapidity (up to $Y \sim 3$, see Fig. 3a). This reflects the known fact that at sufficiently large initial temperatures the contributions of the later stage become negligible. As a result the suppression of the total yield (i.e., plasma and mixed) due to baryon charge becomes larger (by about an order of magnitude, see Fig. 3b). Fig. 3b displays the total yield from quark-gluon matter for the two different initial temperatures and demonstrates the effect of the baryon chemical potential. Similar to the finding in Fig. 2 one observes for $|Y| > 2$ a distinct suppression effect due to the chemical potential.

To measure the initial temperature dependence on the rapidity one can utilize the spectrum $dN/dM^2\, dY$ as function of invariant mass, see Fig. 4. The different slopes of the thermal spectrum reflect the different initial temperatures of the system in the wide rapidity range. M should be high enough to provide the dominant contribution from quark-gluon plasma over the hadronic contributions. On the other hand at large enough M the Drell-Yan background ultimately dominates the spectrum.

The comparison between rapidity distributions of thermal dileptons and the Drell-Yan background for RHIC Au + Au collisions is presented in Fig. 5 for the invariant masses $M = 2, 3$ GeV, respectively, and for $\tau_0 = 0.25$ fm/c. One observes that the central rapidity region is the most appropriate one for the identification of the thermal dilepton production against the hard background. While the Drell-Yan rapidity distribution stays approximately constant in a wide range up to the kinematical limit, the thermal yield from quark-gluon plasma suffers a considerable

suppression at higher rapidities due to the specific initial distribution of temperature and non-zero baryon chemical potential. The range of the rapidity interval, where the quark-gluon yield dominates, depends sensitively on the invariant pair mass and, of course, on the initial temperature of the plasma. We again emphasize that an initial temperature in the order 400 - 500 MeV is necessary to get a dominant plasma contribution over the Drell Yan background in the rapidity interval $|Y| \lesssim 2.5$ at RHIC (see also Ref. [9]).

In order to enhance the difference of the rapidity dependences of the thermal and Drell-Yan pairs it is convenient to employ the correlation between dilepton yield and pion rapidity density [7, 22]

$$K(Y) = A^{2/3} \frac{dN_{l\bar{l}}}{dM^2 \, dY} \left(\frac{dN_\pi}{dY} \right)^{-2} . \tag{16}$$

Since the dilepton yield from the thermal source at high enough initial temperature is proportional to $(dN_\pi/dy)^2$ [4, 5, 7] the function K has for dominating thermal pairs a plateau in the very central rapidity region and decreases with increasing rapidity, see Fig. 6. At the same time the hard dilepton production in central AA collisions probably only weakly depends on the multiplicity of secondary pions (at given bombarding energy) [21, 22]. As a result we find a qualitatively different behavior of the function K for pairs from a thermalized source and those from initial hard parton collisions. Experimentally, one should observe a wide plateau if thermal dileptons dominate, as seen in Fig. 6. In the contrary case of overall dominating Drell-Yan contribution the correlation increases up to a region near the kinematic boundary.

These variations in the rapidity dependence of the scaled yield $K(Y)$ might be useful for the experimental discrimination of the thermal dileptons against Drell-Yan pairs. Although shadowing effects [23] are not taken into account explicitly in our estimates for the Drell-Yan background we can argue that the increase of the function $K(Y)$ with increasing rapidity for the Drell-Yan process will be even stronger due to the shadowing of the nuclear structure functions in the small rapidity region.

Additionally to the Drell-Yan background the decays of charm particles generate also important contributions to the dilepton spectrum for moderately high invariant

10

pair masses. At the same time the kinematics of the charm decays differs from that of thermal or Drell Yan dileptons [9]. This, in principle, allows to subtract the charm background.

We also have found that for these high initial temperatures of the quark-gluon plasma considered above, the contributions from the hadron gas are negligible for $M > 2$ GeV, even when replacing the standard process $\pi^+\pi^- \rightarrow \rho \rightarrow \mu^+\mu^-$ by an effective formfactor which accounts for the numerous other hadronic reactions producing dileptons according to Ref. [18]. Note that also the transverse expansion diminishes the life time of the hadronic phase and suppresses the hadron gas contributions.

V. Summary

In summary, we analyzed the influence of a non-vanishing baryon charge on the rapidity distribution of dileptons in ultrarelativistic heavy-ion collisions. Predictions of microscopic transport simulations for the rapidity distribution of secondary pions and baryons in central collisions at RHIC energies are taken into account. The space time history of the hadronizing quark-gluon plasma includes the mixed phase in the framework of the frozen motion model with scaling expansion. We find a considerable suppression of the dilepton yield due to a large baryon chemical potential that is expected at large rapidities in future RHIC experiments. In the case of SPS energies where the rapidity distribution of baryons is expected to resemble the one of pions with maximum at midrapidities our analysis results in only minor suppression even in the central region. The width of the rapidity interval for observing thermal dileptons over the Drell-Yan background depends strongly on the achieved initial temperature of deconfined matter and the rapidity distribution of baryons. For future RHIC experiments such a useful interval is shown to be restricted by $|Y| \leq 2.5$ if the initial temperature is not below 400 MeV. We propose to use the shape of the scaled dilepton rapidity dependence $K(Y)$ to discriminate thermal dileptons from Drell-Yan background, because the slope of this function is different for both processes.

One can expect that also more involved models with expansion driven by thermodynamical pressure and a sophisticated freeze-out prescription might modify some

11

details of our considerations, but the qualitative features of our results should persist.

References

[1] E.V. Shuryak, Phys. Lett. **B78** (1978) 150

[2] G. Domokos, J.I. Goldman, Phys. Rev. **D23** (1981) 203

[3] P.V. Ruuskanen, in *Quark-Gluon Plasma*, World Scientific, Singapore 1990, edited by R. Hwa, p. 519

[4] L. McLerran, T. Toimela, Phys. Rev. **D31** (1985) 545
R. Hwa, K. Kajantie, Phys. Rev. **D32** (1985) 1109

[5] K. Kajantie, J. Kapusta, L. McLerran, A. Mekjian, Phys. Rev. **D34** (1986) 2746
K. Kajantie, M. Kataja, L. McLerran, P.V. Ruuskanen, Phys. Rev. **D34** (1986) 811

[6] J. Kapusta, L. McLerran, D.K. Srivastava, Phys. Lett. **B283** (1992) 145
B. Kämpfer, O.P. Pavlenko, Phys. Lett. **B289** (1992) 127
K. Geiger, J.I. Kapusta, Phys. Rev. Lett. **70** (1993) 1920
E. Shuryak, L. Xiong, Phys. Rev. Lett. **70** (1993) 2241

[7] M.I. Gorenstein, O.P. Pavlenko, Z. Phys. **C37** (1988) 611
B. Kämpfer, M.I. Gorenstein, O.P. Pavlenko, Z. Phys. **C45** (1990) 491

[8] D. Röhrich (NA35 collaboration) Nucl. Phys. **A566** (1994) 35c

[9] R. Vogt, B.V. Jacak, P.L. McGaughey, P.V. Ruuskanen, Phys. Rev. **D49** (1994) 3345

[10] H. Sorge, H. Stöcker, W. Greiner, Nucl. Phys. **A498** (1989) 567c
H. Sorge, A. Jahns, L. Winckelmann, R. Mattiello, T. Schönfeld, H. Stöcker, W. Greiner, NATO ASI **B303** (1993) p. 335, Plenum Press, New York & London, (Eds.) H.H. Gutbrod, J. Rafelski

[11] H.J. Möring, J. Ranft, Z. Phys. **C52** (1991) 643

[12] A. Dimitru, D.H. Rischke, Th. Schönfeld, L. Winckelmann, H. Stöcker, W. Greiner, Phys. Rev. Lett. **70** (1993) 2860

[13] K. Geiger, J.I. Kapusta, Phys. Rev. **D47** (1993) 4905

[14] U. Heinz, P.R. Subramanian, H. Stöcker, W. Greiner, J. Phys. **G12** (1986) 1237

[15] J. Cleymans, K. Redlich, H. Satz, E. Suhonen, Z. Phys. **C33** (1986) 151

[16] D.H. Rischke, M.I. Gorenstein, J. Stalnacke, E. Suhonen, Z. Phys. **C51** (1991) 485
J. Cleymans, M.I. Gorenstein, J. Stalnacke, E. Suhonen, Phys. Scripta **48** (1993) 277

[17] K.A. Bugaev, M.I. Gorenstein, B. Kämpfer, V.I. Zhdanov, Phys. Rev. **D40** (1989) 2903

[18] D.K. Srivastava, J. Pan, V. Emel'yanov, C. Gale, Phys. Lett. **B329** (1994) 157
E.V. Shuryak, L. Xiong, preprint SUNY-NTG-14 (1994)

[19] B. Kämpfer, O.P. Pavlenko, Z. Phys. **C62** (1994) 491

[20] J.F. Owens, Phys. Lett. **B266** (1991) 126

[21] K. Kajantie, P.V. Ruuskanen, Z. Phys. **C44** (1989) 167

[22] B. Kämpfer, O.P. Pavlenko, Phys. Lett. **B255** (1991) 503

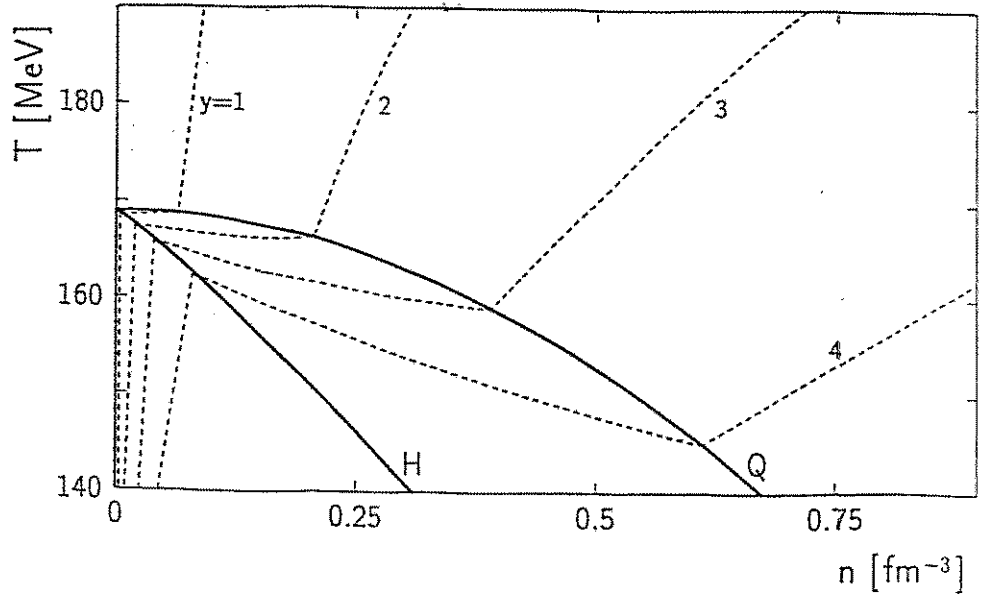[23] L. Frankfurt, M. Strikman, Phys. Rep. **160** (1988) 235

Fig. 1: A section of the phase diagram in the temperature density plane (Q, H - quark-gluon, hadron gas phase boundaries). Dashed lines depict the paths of matter elements with rapidities $y = 1, 2, 3, 4$, respectively.
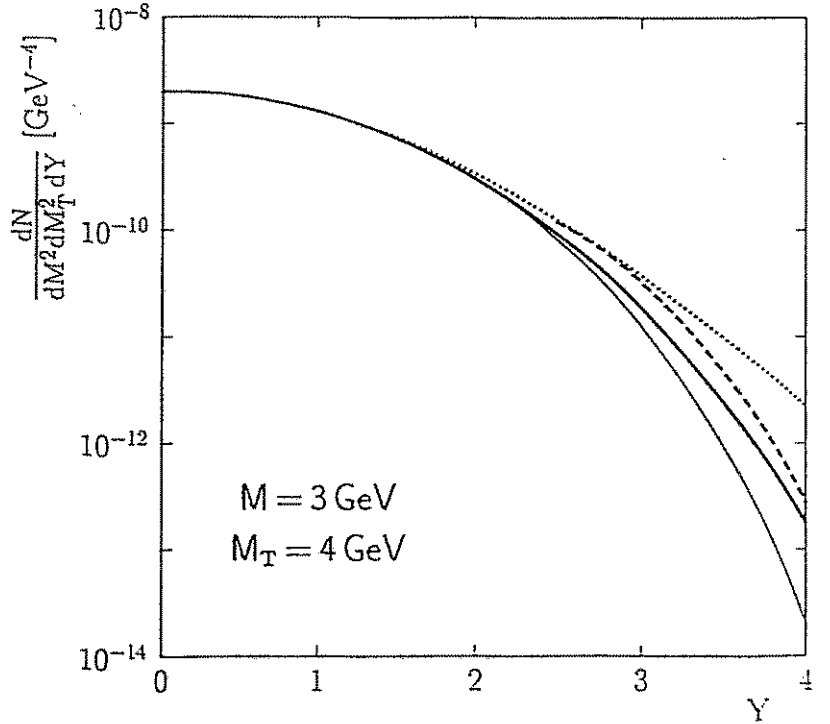

Fig. 2: The rapidity distribution of the dilepton yield $dN_{l\bar{l}}/dM^2\,dM_\perp^2\,dY$ for $M = 3$ GeV and $M_\perp = 4$ GeV. Initial conditions are $\tau_0 = 1$ fm/c and $R = 5$ fm. Heavy full line - plasma + mixed contribution, thin line - only plasma contribution [both with finite chemical potential]; dashed/dotted lines - plasma/plasma + mixed yield [neglecting the baryon chemical potential].
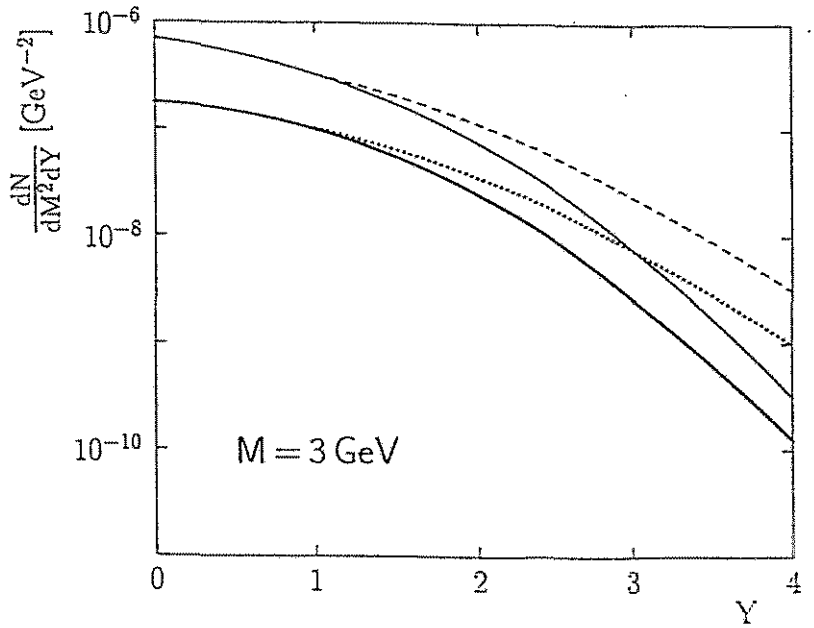
14

Fig. 3a
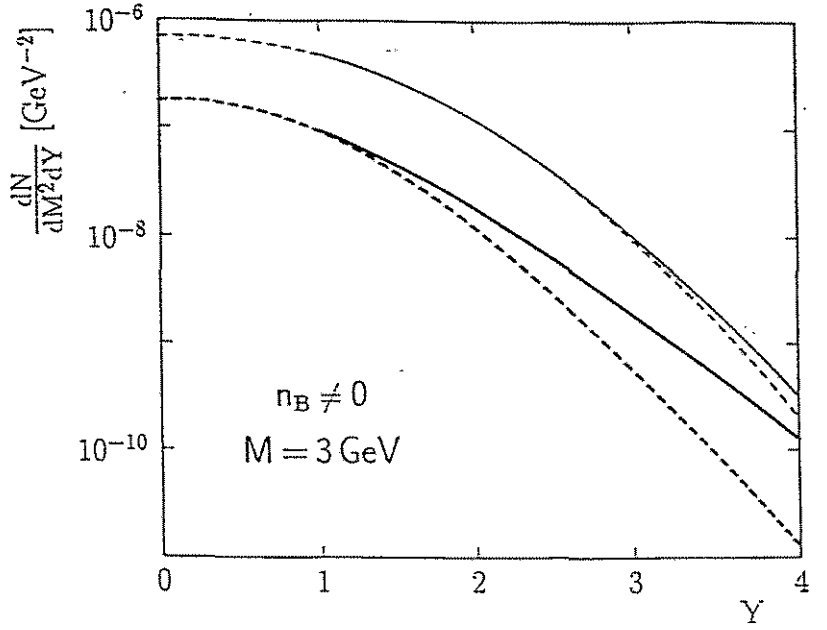
Fig. 3b

Fig. 3: The same as Fig. 2 but the spectrum $dN_{l\bar{l}}/dM^2\,dY$ for $M = 3$ GeV is depicted.

a: For our baryon rapidity distribution and two different initial times τ_0 (long-dashed/heavy full lines - plasma/plasma + mixed contributions for $\tau_0 = 1$ fm·c^{-1}; short-dashed/thin lines - plasma/plasma + mixed contributions for $\tau_0 = 0.5$ fm/c).

b: Comparison of our rapidity distribution with the case of neglecting baryons (heavy full/thin lines - plasma + mixed for $\tau_0 = 1./0.5$ fm·c^{-1} with regard of the finite chemical potential μ_B; dotted/dashed lines - plasma + mixed yield for $\tau_0 = 1./0.5$ fm·c^{-1} and neglecting the baryon chemical potential, i.e., $\mu_B = 0$).
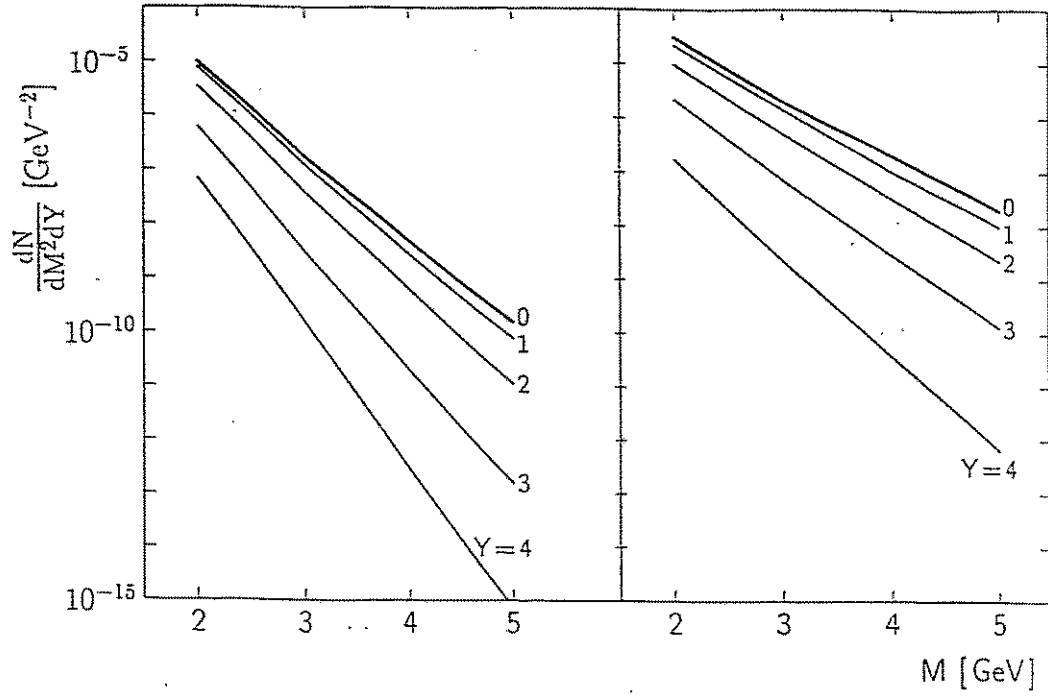
15

Fig. 4: The thermal mass spectrum $dN_{l\bar{l}}/dM^2\,dY$ at various rapidities (left/right panel - $\tau_0 = 1/0.25$ fm·c^{-1}).
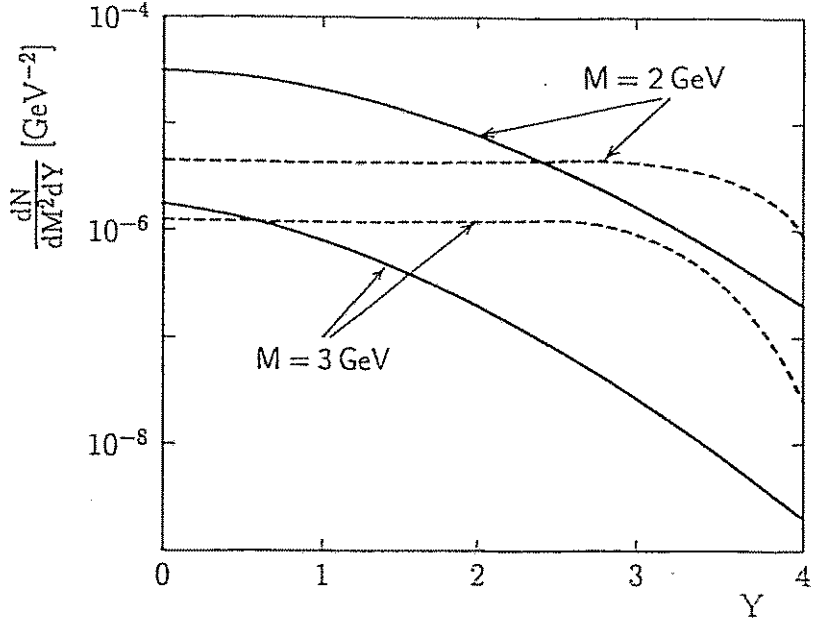

Fig. 5: Rapidity distribution of the yield $dN_{l\bar{l}}/dM^2\,dY$ for $M = 2$ and 3 GeV (full lines). The initial conditions are fixed by $\tau_0 = 0.25$ fm/c. The dotted line depicts the Drell-Yan background for central Au + Au collisions at $\sqrt{s} = 200$ GeV according to eq. (15).

Fig. 6
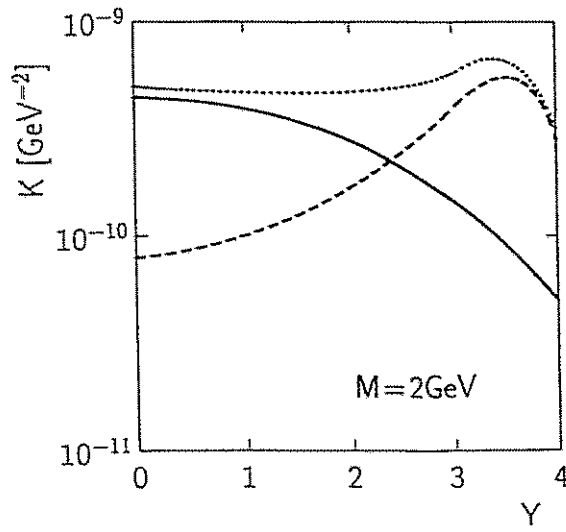
Fig. 6: The correlation function $K(Y)$ for $M = 2$ GeV (Heavy line - thermal contribution, dashed line - Drell-Yan background, dotted line - sum of all contributions).